Available online at www.sciencedirect.com
ScienceDirect
Physics Letters A 366 (2007) 480–486
PHYSICS LETTERS A
www.elsevier.com/locate/pla

Electromechanical nanothermometer

Elena Bichoutskaia [a], Andrey M. Popov [b], Yurii E. Lozovik [a,*], Gennadii S. Ivanchenko [c], Nikolai G. Lebedev [c]

[a] *University Chemical Laboratory, Lensfield road, Cambridge CB2 1EW, UK*
[b] *Institute of Spectroscopy, Troitsk, Moscow Region 142190, Russia*
[c] *Volgograd State University, University Avenue 100, Volgograd 400062, Russia*

Received 2 December 2006; accepted 8 January 2007

Available online 21 February 2007

Communicated by V.M. Agranovich

Abstract

A new concept of an electromechanical nanothermometer based on the interaction and relative motion of the components of a nanosystem is proposed. The nanothermometer can be used for accurate temperature measurements in spatially localized regions with dimensions of several hundred nanometers. Temperature measurements are carried out through the measurements of the conductivity of the components assuming that the total conductivity of the system depends significantly on the temperature. A model implementation of the nanothermometer based on the (6, 6)@(11, 11) double-walled carbon nanotube is suggested. The dependence of the interwall interaction energy on the relative displacement of the walls of the (6, 6)@(11, 11) nanotube is computed *ab initio* using density functional theory. The conductivity of the walls is calculated within the Huckel–Hubbard model.

PACS: 61.46.Fg; 85.85.+j

Keywords: Nanotube; Nanodevice; Nanothermometer; NEMS

1. Introduction

With the considerable progress in nanotechnology techniques, a number of feasible designs of nanoelectromechanical systems (NEMS) have recently evolved, in which the elements of electric circuits represent nanoobjects of progressively smaller scale reaching the size of a single molecule. The operation of some NEMS is based on the changes in electronic structure and conductivity of a system due to the change in the relative position of its components at subnanometer scale [1–3]. A few examples of such NEMS based on carbon nanotubes such as a variable nanoresistor [4–6], a strain nanosensor [7] and a nonvolatile memory element [8] have already been conceptualized and simulated.

In this Letter, a new concept of an electromechanical nanothermometer based on the interaction and relative motion of the components of a nanosystem is proposed. It rests on the measurements of the conductivity of the components which, under the certain conditions, depends on their relative positions. The total conductivity of a system then changes significantly with the temperature due to the thermal vibrations of the components.

In general, the temperature dependence of the total conductivity $G(T)$ of a system can be expressed as

$$G(T) = \frac{\int_{-\infty}^{\infty} G(q,T)\exp(-U(q)/kT)\,dq}{\int_{-\infty}^{\infty}\exp(-U(q)/kT)\,dq}, \tag{1}$$

where $G(q,T)$ is the conductivity of the system at a fixed relative position of the components which are defined by the coordinates q; $U(q)$ is the potential energy of the system. Eq. (1) takes into account the contributions from the thermal vibration of the components. Any nanosystem can be used as an electro-

* Corresponding author. Tel.: +7 495 334 0881; fax: +7 495 334 0886.
E-mail address: lozovik@isan.troitsk.ru (Yu.E. Lozovik).

0375-9601/$ – see front matter
doi:10.1016/j.physleta.2007.01.077

mechanical nanothermometer if it complies with the following requirements:

(1) the 'local' conductivity $G(q,T)$ depends significantly on the coordinates q (condition A);
(2) $G(q,T)$ depends weakly on the temperature T at a fixed position of the constituent components (condition B);
(3) the amplitude of the thermal vibrations of the components is large enough to provide the main contribution to the temperature dependence of the total conductivity $G(T)$ (condition C);
(4) the amplitude of the thermal vibrations of the components is still small for the relative displacements of the components to upset the normal operation of the system (condition D).

The conditions B and C imply that the contributions to $G(T)$ from phenomena other than the thermal vibrations of the components are insignificant. It is also desirable, although not necessary, that the minimum of the potential energy curve $U(q)$, near which the thermal vibrations of the components occur, coincide with the extremum in the dependence of the conductivity on the coordinate $G(q)$ (condition E). The condition E ensures that the contributions to the change in the conductivity from the vibrations corresponding to different displacements from the equilibrium position of the system are not cancelled out. If the condition E is fulfilled, any small displacements lead to the changes of the same sign (either decrease or increase of the conductivity). The minimum of $U(q)$ and the extremum of $G(q)$ coincide if, for example, the equilibrium position corresponds to a high symmetry of the system.

The conditions A–E can be satisfied if the nanothermometer is built using double-walled carbon nanotubes (DWNTs) with nonchiral commensurate walls. Recent studies show that the conductivity of DWNTs depends on the relative position of the walls [9–11]. In the telescopic systems, in which a small-diameter single-walled carbon nanotube (SWNT) is inserted a certain distance into a larger diameter SWNT, the overlap of the walls is always less than the lengths of the constituent SWNTs. In the shuttle structures, in which a large-diameter SWNT (a shuttle) is placed outside a small-diameter inner-wall SWNT, the overlap of the walls is equal to the length of the shuttle.

For both telescopic and shuttle systems, dependence of the 'local' conductivity on the displacement z of the walls, $G(z)$, is a periodic function with large oscillations [10,11]. This result ensures that the condition A is fulfilled. For telescopic DWNTs, the conductivity also depends on the length of the overlap of the walls [11,12]. First experimental measurements of the temperature dependence of the resistance of SWNTs have been reported recently [13]. These measurements show that the resistance of SWNTs does not change for the temperatures above 80 K. The weak temperature dependence of the conductivity is due to the ballistic transport over mesoscale distances [14]. Calculations presented in this Letter for the conductivity of DWNTs with the fixed position of the walls show very weak temperature dependence above 50 K. These results yield the fulfillment of the condition B. The relative position of the walls of DWNT changes due to the thermal vibration of the walls. Therefore, the total conductivity of DWNT depends significantly on the temperature, and, mainly, as a result of the thermal vibration. The dependence of the interwall interaction energy of DWNTs on the relative displacement of the walls is calculated *ab initio*. For the nanothermometer based on DWNTs, this dependence is subsequently used to estimate the possibility of fulfillment of the conditions C and D, as well as the minimum dimensions of the nanothermometer for which the relative diffusion of the walls does not hinder its operation. Analysis of the symmetry of DWNTs shows that the condition E is also satisfied for the nanothermometer based on DWNTs.

Experimental measurements of the conductivity of individual carbon nanotubes [15,16], together with the advances in syntheses of DWNTs [17–20], make our conceptual design realistic within the available nanotechnology. The general concept described above stimulates the search for a wider range of nanosystems suitable for using as an electromechanical nanothermometer.

2. Calculation of the interwall interaction energy

The interwall interaction energy of DWNT depends on the relative position of the walls. This position can be described by ϕ, the angle of relative rotation of the walls about the longitudinal axis of DWNT, and z, the relative displacement of the walls along this axis. The symmetry of the interwall interaction energy surface, as well as the relative position of the walls corresponding to the extrema of the surface, are uniquely determined by the symmetry of DWNT [21,22]. For the $(n,n)@(m,m)$ armchair and $(n,0)@(m,0)$ zigzag DWNTs, the Fourier expansion of the interwall interaction energy is given in [21] as

$$U(\phi,z) = \sum_{M,K\,(\mathrm{odd})=1}^{\infty} \alpha_K^M \cos\left(\frac{2\pi}{l_c}Kz\right)\cos\left(\frac{nm}{N}M\phi\right) \times \sin^2\left(\frac{\pi nm}{2N^2}\right) + \sum_{M,K\,(\mathrm{even})=0}^{\infty} \beta_K^M \cos\left(\frac{2\pi}{l_c}Kz\right) \times \cos\left(\frac{nm}{N}M\phi\right), \quad (2)$$

where N is the greatest common factor of n and m, and l_c is the length of the unit cell of DWNT. The even terms are always present in Eq. (2), and the odd terms only occur if both $\frac{n}{N}$ and $\frac{m}{N}$ are odd. According to the topological theorem [23], extrema of the interaction energy surface of DWNT correspond to the positions of the walls for which the second-order symmetry axes of the inner and outer walls are in line. These axes are perpendicular to the principal symmetry axis of the wall and pass through either the mid-point of the carbon bond or the centre of hexagons. The points on the surface which correspond to the extrema are called critical points (ϕ_c, z_c) of the interwall interaction energy surface. For the armchair $(n,n)@(m,m)$ and zigzag $(n,0)@(m,0)$ DWNTs, the elementary cell of $U(\phi,z)$ contains four types of critical points (ϕ_c, z_c)—a minimum, a maximum and two saddle points.

The amplitude of harmonics in expansion (2) drops rapidly as parameters M and K increase [22–24]. For DWNTs with nonchiral commensurate walls, $U(\phi, z)$ can be interpolated using the first two harmonics of the expansion (2)

$$U(\phi, z) = U_0 - \frac{\Delta U_\phi}{2}\cos\left(\frac{2\pi}{\delta_\phi}\phi\right) - \frac{\Delta U_z}{2}\cos\left(\frac{2\pi}{\delta_z}z\right), \qquad (3)$$

where U_0 is the average interwall interaction energy, ΔU_ϕ and ΔU_z are the energy barriers to rotation and sliding of the walls, and δ_ϕ and $\delta_z = l_c/2$ are the periods of rotation and sliding of the walls between the equivalent positions. Semiempirical calculations [25] show that expansion (3) holds for $U(\phi, z)$ within the accuracy of 1% of the values of ΔU_ϕ and ΔU_z. *Ab initio* results [26] for the $(5, 5)@(10, 10)$ DWNT suggest that $U(\phi, z)$ can be interpolated using expansion (3) within the accuracy of 5% of the value of the energy barriers.

For DWNTs with incompatible rotational symmetries of nonchiral commensurate walls, calculations [25] and [27] of the interwall interaction energy surfaces and calculations [10] of the conductivity of DWNTs show that the dependence of both the interwall interaction energy and the conductivity on ϕ is negligible. Neglecting the ϕ dependence in (3), the interwall interaction energy can be written as

$$U(z) = U_0 - \frac{\Delta U_z}{2}\cos\left(\frac{2\pi}{\delta_z}z\right). \qquad (4)$$

Expressions (2)–(4) are valid for any property of DWNT which depends on the relative positions of the walls. It is particularly true for the conductivity $G(\phi, z)$, as both functions $U(\phi, z)$ and $G(\phi, z)$ have the same periods δ_ϕ and δ_z and the same number of harmonics. Furthermore, extrema of $U(\phi, z)$ and $G(\phi, z)$ coincide, and the dependence of $U(\phi, z)$ and $G(\phi, z)$ on ϕ is negligible in the case of incompatible rotational symmetries of the walls. Thus, the condition E is satisfied for the nanothermometer based on DWNT.

The interwall interaction energy $U(\phi, z)$ has been calculated for the $(6, 6)@(11, 11)$ DWNT which has incompatible rotational symmetry of the constituent walls. The density functional AIMPRO supercell code [28] within the local density approximation has been used. Within AIMPRO, the pseudowave functions are described by 4 atom-centered Gaussian functions per atom expanded in spherical harmonics up to $l = 1$, with the second smallest exponent expanded to $l = 2$. The supercell consists of 68 carbon atoms. The Brillouin Zone sampling has been performed using 18 special k-points in the direction of the nanotube axis. Non-local, norm-conserving pseudopotential [29] and the Perdew–Wang exchange–correlation functional [30] have been used. Minima in the total energy have been found using a conjugate gradient scheme to the accuracy of 1 μeV/atom. Positions of all atoms in the isolated $(6, 6)$ and $(11, 11)$ SWNTs have been optimized. The interwall interaction energy has been calculated as the difference between the total energy of the $(6, 6)@(11, 11)$ DWNT and the separate $(6, 6)$ and $(11, 11)$ SWNTs.

$U(\phi, z)$ has been calculated as a function of relative displacement of the walls along the principal axis of the DWNT, i.e. at a fixed angle ϕ and five values of z including two critical points which correspond to the minimum and maximum of $U(\phi, z)$. The minimum of $U(\phi, z)$ corresponds to the relative position of the walls for which the second-order symmetry axes of the inner and outer walls are in line and pass through the mid-point of the carbon bond. In order to calculate the barrier to relative sliding of the walls, the dependence $U(z)$ has been interpolated using Eq. (4) within the accuracy of the calculations. The accuracy of the calculations has been estimated using the difference between the values of $U(z)$ calculated in the equivalent positions of the walls as described in [27].

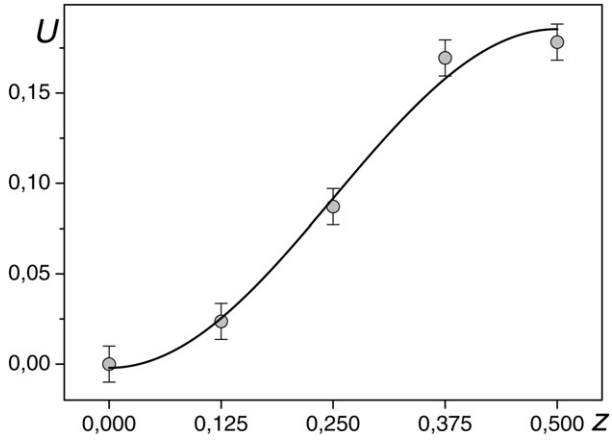

Fig. 1. The interwall interaction energy (in meV per atom of the outer wall) of the $(6, 6)@(11, 11)$ DWNT as a function of the displacement of the walls. The displacement z is measured in units of the period δ_z of the interwall interaction energy as a function of the relative sliding of the walls. The calculated values of the energy are shown by circles. The solid line is the interpolation of the energy using expansion (4). The minimum of the interwall interaction energy is positioned at $U = 0$ and $z = 0$.

Fig. 1 shows the calculated values of $U(z)$ for the $(6, 6)@(11, 11)$ DWNT and the interpolation curve. The barrier to relative sliding of the walls of the $(6, 6)@(11, 11)$ DWNT obtained from the interpolation curve is 0.187 ± 0.10 meV per atom of the outer wall.

3. Calculation of the conductivity

The conductivity of SWNTs with different diameters has been measured experimentally as 100 μSm [31]. This value is of the same order of magnitude as the conductivity quantum, $4e^2/h = 154$ μSm. This suggests the possibility of presence of quantum effects in some temperature intervals which may account for the phase transitions such as metal—semiconductor transition. To explore this possibility, the conductivity of the $(6, 6)@(11, 11)$ DWNT has been calculated using the Huckel–Hubbard model described in [32]. The model Hamiltonian includes the energy of an electron travelling between the neighbouring carbon atoms, as well as between the walls of DWNT, and the energy of Coulomb interaction of electrons located at the same lattice point

$$\hat{H} = -\sum_{j\Delta\sigma} t^a_\Delta \left(a^+_{j\sigma}a_{j+\Delta\sigma} + a^+_{j+\Delta\sigma}a_{j\sigma}\right) - \mu^a \sum_{j\sigma} a^+_{j\sigma}a_{j\sigma} + U\sum_j a^+_{j\sigma}a_{j\sigma}a^+_{j-\sigma}a_{j-\sigma}$$

$$- \sum_{j\Delta\sigma} t_{\Delta}^{b}\left(b_{j\sigma}^{+} b_{j+\Delta\sigma} + b_{j+\Delta\sigma}^{+} b_{j\sigma}\right)$$
$$- \mu^{b} \sum_{j\sigma} b_{j\sigma}^{+} b_{j\sigma} + U \sum_{j} b_{j\sigma}^{+} b_{j\sigma} b_{j-\sigma}^{+} b_{j-\sigma}$$
$$- \sum_{j\zeta\sigma} t_{\zeta}^{ab}\left(a_{j\sigma}^{+} b_{j+\zeta\sigma} + b_{j+\zeta\sigma}^{+} a_{j\sigma}\right), \tag{5}$$

where a^{+}, a, b^{+}, b are the operators of creation and annihilation of an electron with the spin σ located at the lattice point j of the inner and outer wall; t_{Δ}^{a}, t_{Δ}^{b}, and t_{ζ}^{ab} are the integrals describing the motion of an electron within the inner and outer walls and between the walls; U is the Coulomb repulsion energy of electrons at the lattice point j; μ^{a} and μ^{b} are the chemical potentials of the inner and outer walls. The conductivity tensor has been calculated using Green's functions of the Heisenberg equation for the operators of creation and annihilation according the Kubo formula [34]

$$G_{\alpha\beta} = \frac{i\pi V}{kT} \langle\langle j_{\alpha} | j_{\beta} \rangle\rangle, \tag{6}$$

where V is the volume of DWNT, T is the absolute temperature, $\langle\langle j_{\alpha} | j_{\beta} \rangle\rangle$ is the retarded Green's function of the current density, and α and β are the component indices of the current density vector $\hat{\mathbf{j}}$. The vector $\hat{\mathbf{j}}$ is defined as

$$\hat{\mathbf{j}} = \frac{ie}{V} \sum_{k\sigma} \left[\left(\mathbf{v}^{a} a_{k\sigma}^{+} a_{k\sigma} + \mathbf{v}^{b} b_{k\sigma}^{+} b_{k\sigma}\right) + \mathbf{v}^{ab}\left(b_{k\sigma}^{+} a_{k\sigma} + a_{k\sigma}^{+} b_{k\sigma}\right)\right]. \tag{7}$$

$\mathbf{v}^{a}$, $\mathbf{v}^{b}$ and $\mathbf{v}^{ab}$ are velocities of an electron in inner a, outer b and inter ab bands, i.e.

$$\mathbf{v}^{a} = \frac{1}{\hbar} \frac{\partial \varepsilon^{a}(\mathbf{k})}{\partial \mathbf{k}}, \qquad \mathbf{v}^{b} = \frac{1}{\hbar} \frac{\partial \varepsilon^{b}(\mathbf{k})}{\partial \mathbf{k}},$$
$$\mathbf{v}^{ab} = \frac{1}{\hbar} \frac{\partial \varepsilon^{ab}(\mathbf{k})}{\partial \mathbf{k}}, \tag{8}$$

where ε^{a}, ε^{b}, and ε^{ab} are dispersion relations of an electron in a, b and ab bands.

Calculation of the isotropic conductivity as a function of the temperature has been described in detail elsewhere [33]. For a number of DWNTs, a wide plateau in the temperature dependence of the total conductivity $G(T)$ has been reported in the interval from 5 to 300 K [33]. However, in [33] the effects associated with the finite length of the walls of DWNT have been neglected. In this Letter, $G(T)$ has been calculated for three lengths of the movable outer (11, 11) wall, namely 30, 100 and 1000 unit cells of the (6, 6)@(11, 11) DWNT. Fig. 2 shows a very weak temperature dependence of the conductivity above 50 K for the curves which correspond to the lengths of 30 and 100 unit cells. The curve which corresponds to 1000 unit cells is indistinguishable from the curve for 100 unit cells. This implies that the contributions to the total conductivity from phenomena other than the thermal vibration of the walls are insignificant (fulfillment of the condition B).

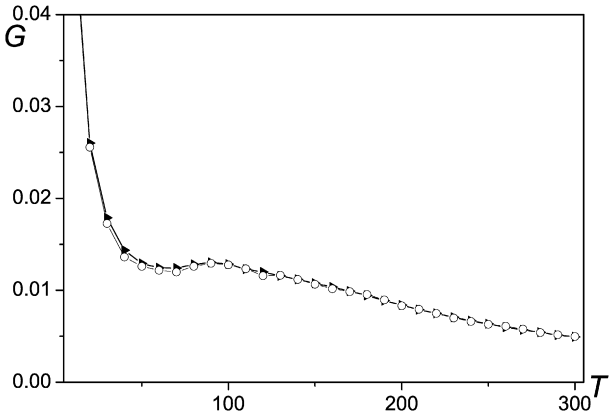

Fig. 2. The conductivity (in Sm/m) as a function of the temperature (in Kelvin degrees) calculated for two lengths of the movable outer wall: 30 (open circles) and 100 (filled triangles) lengths of the unit cell of the (6, 6)@(11, 11) DWNT.

4. Basic design of a nanothermometer

Fig. 3 is a schematic which shows a shuttle nanothermometer with a short movable outer wall (the shuttle) (Fig. 3A) and a telescopic nanothermometer with a movable inner wall (Fig. 3B). A shuttle nanothermometer with a movable inner wall and a telescopic nanothermometer with a movable outer wall are also possible.

Due to the symmetry of DWNT, the extrema of $U(z)$ and $G(z, T)$ coincide. As discussed in Section 2, the $U(z)$ curve can be interpolated near the bottom of the potential well as

$$U(z') = U_1 + \frac{\pi \Delta U_z}{\delta_z^2} z'^2, \tag{9}$$

where U_1 is the interwall interaction energy of DWNT in the ground state and z' is the displacement of the movable wall from the position which corresponds to the ground state. For small values of z', $G(z', T)$ can be interpolated as

$$G(z') = G_1(T)\left(1 + \gamma z'^2\right), \tag{10}$$

where G_1 is the conductivity of DWNT in the ground state.

Substitution of (9) and (10) into (1) leads to the following expression for the dependence of the conductivity of the nanothermometer on the temperature

$$G(T) = G_1(T)\left(1 + \frac{\gamma \delta_z^2 kT}{\pi \Delta U_z}\right) = G_1(T)(1 + HT). \tag{11}$$

The condition C for the successful operation of the nanothermometer, which states that the thermal vibrations give the main contribution to the dependence of the conductivity on the temperature is fulfilled if

$$H\Delta T \gg \frac{\Delta G_1(T)}{\langle G_1(T) \rangle}, \tag{12}$$

where $\Delta G_1(T)$ is the difference between the minimum and maximum values of the conductivity of DWNT in the ground state in the temperature range that can be measured by the nanothermometer; $\langle G_1(T) \rangle$ is the mean conductivity of the nanothermometer in this temperature range ΔT. It can be extracted from Fig. 2 that in the temperature range $\Delta T = 250$ K, the ratio

Fig. 3. Schematic of an electromechanical nanothermometer. A: the telescopic nanothermometer with the movable inner wall, B: the shuttle nanothermometer with the movable outer wall. The movable wall is indicated as (1), the fixed wall as (2) and the attached electrodes as (3).

in formula (12) is approximately unity, i.e.

$$\frac{\Delta G_1(T)}{\langle G_1(T)\rangle} \sim 1. \tag{13}$$

In order to estimate the possibility of fulfillment of the condition C for the nanothermometer based on the $(6,6)@(11,11)$ DWNT, the interwall interaction energy $U(z)$ calculated in Section 2 has been used together with the results of [10] for the conductivity of this DWNT. The dependence of the conductivity on the relative displacement of the walls for the telescopic system (Fig. 3 of [10]) has been interpolated near the minimum using expression (10), and the following estimates for γ have been obtained for the $(6,6)@(11,11)$ DWNT: $\gamma = 855 \pm 124$ Å^{-2} for the overlap of the walls of 10 unit cells in length and $\gamma = 21 \pm 12$ Å^{-2} for the overlap of 250 unit cells. According to the *ab initio* calculations of Section 2, the barriers to the relative sliding of the movable wall are $\Delta U_z = 78.4$ meV and $\Delta U_z = 1.96$ eV for the overlap of the walls of 10 and 250 unit cells, respectively. If $\Delta T = 250$ K, the value of $H\Delta T$ acquires the following values: 117 ± 17 for the overlap of 10 unit cells and 0.43 ± 0.10 for the overlap of 250 unit cells. Thus, the condition C is satisfied for small overlaps of the walls.

The minimum dimensions of the nanothermometer for which the condition D can be fulfilled have been also estimated. The condition D states that the amplitude of the thermal vibrations of the movable wall has to be relatively small so that these vibrations do not upset the normal operation of the nanothermometer. It is clear that the shorter the movable wall is, the larger the amplitude of the vibrations of this wall become. In principle, the diffusion of the shuttle along the fixed wall can occur. This is an undesirable process which can hinder the operation of the nanothermometer, and it needs to be prevented.

For the shuttle design (Fig. 3A), the displacement d of the shuttle (1) must be less than the distance L_{es} between the electrode (3) and the shuttle in any given time t of the operation of the nanothermometer, i.e.

$$d = \sqrt{2Dt} < L_{es}, \tag{14}$$

where D is the diffusion coefficient for the motion of the shuttle along the fixed wall (2). Expression for the diffusion coefficient D has been given in [26] as follows

$$D = A\exp\left(-\frac{BL}{T}\right), \quad A = \pi\delta_z\sqrt{\frac{\Delta U_z}{2m}}, \; B = \frac{\Delta U_z N_a}{l_m k}, \tag{15}$$

where m is the mass of carbon atom, N_a is the number of atoms in the unit cell of the shuttle, l_m is the length of the unit cell of the shuttle, and L is the length of the shuttle. Thus, the length of the shuttle can be estimated as

$$L = \frac{T}{B}\ln\left(\frac{2At}{L_{es}^2}\right), \tag{16}$$

and the total length L_{nt} of the nanothermometer between the electrodes as

$$L_{nt} = \frac{T}{B}\ln\left(\frac{2At}{L_{es}^2}\right) + 2L_{es}. \tag{17}$$

The total length of the nanothermometer is minimal if $L_{nt} = \frac{T}{B}$. This condition for the minimum total length of the nanothermometer does not depend on the time of its operation. Using the *ab initio* results of Section 2 for the barrier ΔU_z of the $(6,6)@(11,11)$ DWNT, parameter A is found to be $1.05 \pm 0.03 \times 10^{-8}$ m^2/s for the movable outer wall and $1.46 \pm 0.04 \times 10^{-8}$ m^2/s for the movable inner wall. Parameter B has the value of 380 ± 20 K/nm for both the inner and outer walls. At $T = 300$ K, the temperature which corresponds to the plateau on Fig. 2, the length L_{es} is approximately 0.8 nm. This dimension is only three times greater than the translational length of the unit cell of the $(6,6)@(11,11)$ DWNT, $l_c = 0.244$ nm.

Table 1
Characteristics of the nanothermometer based on the $(6,6)@(11,11)$ DWNT with the movable outer wall (shuttle): T (in K) is the temperature of the operation, t (in s) is the time of the operation, L_{nt} (in nm) is the minimal lengths between the electrodes, N_c is the number of unit cells of DWNT corresponding to the length of shuttle

T	t	l_{nt}	N_c
100	10^{-6}	3.8	14
100	100 years	13.1	52
300	10^{-6}	9.8	34
300	100 years	38	149

Table 1 shows the total length of the nanothermometer L_{nt} which operates at the temperatures $T = 100$ K and $T = 300$ K in two different regimes: the permanent mode of the operation during 100 years and the pulse mode with the time of the operation of 10^{-6} s. These dimensions have been estimated using Eq. (17). Since L_{nt} is a logarithmic function of A, the total length of the nanothermometer is approximately the same whether the inner wall is movable or the outer wall. Comparing (16) and (17) and taking into account the estimated values of L_{es} and L_{nt}, it can be concluded that the length of the shuttle is about the same as the total length of the nanothermometer, i.e. $L \approx L_{nt}$.

For the telescopic design (Fig. 3B), the length L in Eq. (16) is the overlap between the movable wall (1) and the fixed walls

(2) connected to the electrodes (3). In this case, the length of the gap between the two fixed walls has to be added to the total length of the nanothermometer. The proposed schematics of the shuttle and telescopic nanothermometers are of a true nanometer size which is governed merely by the length needed to attach the electrodes.

The estimates based on the results of [10] show that the value of $H\Delta T$ is significantly large only for small length of the movable wall (tens of unit cells of DWNT). Thus, the shuttle design of the nanothermometer based on the $(6, 6)@(11, 11)$ DWNT can be used in the permanent mode for the temperature measurements up to 100 K and in the pulse mode for the temperature measurements up to 300 K. According to the *ab initio* results [35], the diffusion coefficient of the nonchiral commensurate movable wall decreases with increasing the radius. It seems plausible that nonchiral commensurate DWNTs with large radii can be used in the nanothermometers which can measure the room temperatures in the permanent regime.

5. Concluding remarks

A new type of an electromechanical nanothermometer which can be used for accurate temperature measurements in spatially localized regions with dimensions of several hundred nanometers has been proposed. The nanothermometer can be calibrated using a thermocouple. Since the temperature measurements are based on the conductivity measurements, the nanothermometer can provide as accurate measurement of the temperature as a thermocouple.

Another type of nanothermometer based on gallium-filled carbon nanotubes has been recently reported [36,37]. In this nanothermometer, the temperature measurements are based on the thermal expansion of a column of liquid gallium inside a carbon nanotube of 10 μm long. This method relies on the identification and calibration of the nanothermometer in a transmission electron microscope. Such shortcoming limits the use of such nanothermometer in nanodevices.

A considerable progress has been recently achieved in the nanotechnology techniques in the field of production of NEMS. A nanomanipulator can be now attached to MWNT in order to move individual walls [38,39], manipulation with SWNTs is routinely possible [39,40], the caps of the walls can be removed [41–43], nanotubes can be cut into pieces of desirable length [44]. Recently, the techniques for unambiguous determination of chirality of the walls have been successfully demonstrated [45]. All these give us a cause for optimism that the proposed new type of the electromechanical nanothermometer will be produced in the near future.

Acknowledgements

E.B. is grateful to The Royal Society for the UK Relocation Fellowship. This work has been partially supported by the Russian Foundation of Basic Research (YEL 06-02-81036-Bel; A.M.P. grant 05-02-17864; G.S.I. and N.G.L. grant 04-03-96501). We are thankful to Prof. M.B. Belonenko for fruitful discussions.

References

[1] H. Park, J. Park, A.K.L. Lim, E.H. Anderson, A.P. Aliviscatos, P.L. McEuen, Nature 404 (2000) 57.
[2] A. Isacsson, T. Nord, Europhys. Lett. 66 (2004) 708.
[3] T. Nord, A. Isacsson, Phys. Rev. B 69 (2004) 035309.
[4] Yu.E. Lozovik, A.V. Minogin, A.M. Popov, Phys. Lett. A 313 (2003) 112.
[5] Yu.E. Lozovik, A.V. Minogin, A.M. Popov, JETP Lett. 77 (2003) 631.
[6] Yu.E. Lozovik, A.M. Popov, Fullerenes Nanotubes Carbon Nanostructures 12 (2004) 485.
[7] E. Bichoutskaia, M.I. Heggie, Yu.E. Lozovik, A.M. Popov, Fullerenes Nanotubes Carbon Nanostructures 14 (2006) 131.
[8] L. Maslov, Nanotechnology 17 (2006) 2475.
[9] A. Hanson, S. Stafström, Phys. Rev. B 67 (2003) 075406.
[10] I.M. Grace, S.W. Bailey, C.J. Lambert, Phys. Rev. B 70 (2004) 153405.
[11] M.A. Tunney, N.R. Cooper, Phys. Rev. B 74 (2006) 075406.
[12] D.H. Kim, K.J. Chang, Phys. Rev. B 66 (2002) 155402.
[13] B. Gao, Y.F. Chen, M.S. Fuhrer, D.C. Glattli, A. Bachtold, Phys. Rev. Lett. 95 (2005) 196802.
[14] M.S. Dresselhaus, G. Dresselhaus, P. Avouris (Eds.), Carbon Nanotubes: Synthesis, Structure, Properties and Applications, Springer, Berlin, 2001.
[15] S.J. Tans, M.H. Devoret, H. Dai, A. Thess, R.E. Smalley, L.J. Geerlings, C. Dekker, Nature 386 (1997) 474.
[16] S.J. Tans, A.R.M. Verschueren, C. Dekker, Nature 393 (1998) 49.
[17] J.L. Hutchison, N.A. Kiselev, E.P. Krinichnaya, A.V. Krestinin, R.O. Loufty, A.P. Moravsky, V.E. Muradyan, E.D. Obraztsova, J. Sloan, S.V. Terekhov, D.N. Zakharov, Carbon 39 (2001) 761.
[18] S. Bandow, M. Takizawa, K. Hirahara, M. Yadasako, S. Iijima, Chem. Phys. Lett. 337 (2001) 48.
[19] E. Flahaut, A. Peigney, C. Laurent, A. Rousset, J. Mater. Chem. 10 (2000) 249.
[20] J. Sloan, M.C. Novotny, S.R. Bailey, G. Brown, C. Xu, V.C. Williams, S. Friedrichs, E. Flahaut, R.L. Callender, A.P.E. York, K.S. Coleman, M.L.H. Green, R.E. Dunin-Borkowski, J.L. Hutchison, Chem. Phys. Lett. 329 (2000) 61.
[21] M. Damnjanović, I. Milošević, T. Vuković, R. Sredanović, Phys. Rev. B 60 (1999) 2728.
[22] T. Vuković, M. Damnjanović, I. Milošević, Physica E 16 (2003) 259.
[23] M. Damnjanović, E. Dobardzić, I. Milošević, T. Vuković, B. Nikolić, New J. Phys. 5 (2003) 148.
[24] M. Damnjanović, T. Vuković, I. Milošević, Eur. Phys. J. B 25 (2002) 131.
[25] A.V. Belikov, Yu.E. Lozovik, A.G. Nikolaev, A.M. Popov, Chem. Phys. Lett. 385 (2004) 72.
[26] E. Bichoutskaia, A.M. Popov, A. El-Barbary, M.I. Heggie, Yu.E. Lozovik, Phys. Rev. B 71 (2005) 113403.
[27] E. Bichoutskaia, A.M. Popov, M.I. Heggie, Yu.E. Lozovik, Phys. Rev. B 73 (2006) 045435.
[28] P.R. Briddon, R. Jones, Phys. Stat. Sol. 217 (2000) 131.
[29] G.B. Bachelet, D.R. Hamann, M. Schlüter, Phys. Rev. B 26 (1982) 4199.
[30] J.P. Perdew, Y. Wang, Phys. Rev. B 45 (1992) 13244.
[31] P.J.F. Harris, Carbon Nanotubes and Relative Structures. New Materials of Twenty-First Century, Cambridge Univ. Press, Cambridge, 1999, p. 336.
[32] A.A. Abrikosov, L.P. Gorkov, I.E. Dzyaloshinskii, Metody Kvantovoi Teorii Polya v Statisticheskoi fizike (Methods of the Quantum Field Theory in Statistical Physics), Dobrosvet, Moscow, 1998, p. 514.
[33] G.S. Ivanchenko, N.G. Lebedev, I.V. Zaporotskova, in: Abstracts of 7th Biennial International Workshop Fullerenes and Atomic Clusters, St.-Peterburg, Russia, 2005, p. 66;
G.S. Ivanchenko, N.G. Lebedev, Phys. Solid State 49 (2000).
[34] Y. Imry, Introduction in Mesoscopic Physics, Oxford Univ. Press, Oxford, 1997, p. 234.
[35] E. Bichoutskaia, M.I. Heggie, Yu.E. Lozovik, A.M. Popov, Fullerenes Nanotubes Carbon Nanostructures 14 (2006) 215.
[36] Y. Gao, Y. Bando, Nature 415 (2002) 599.
[37] Y. Gao, Y. Bando, Z. Liu, D. Golberg, H. Nakanishi, Appl. Phys. Lett. 83 (2003) 2913.
[38] J. Cumings, A. Zettl, Science 289 (2000) 602.

[39] M.F. Yu, M.J. Dyer, G.D. Skidmore, H.W. Rohrs, X.K. Lu, K.D. Ausman, J.R. Von Ehr, R.S. Ruoff, Nanotechnology 10 (1999) 244.
[40] Z. Shen, S. Lie, Z. Xue, Z. Gu, Int. J. Nanosci. 1 (2002) 575.
[41] S.C. Tsang, P.J.F. Harris, M.L.H. Creen, Nature 362 (1993) 520.
[42] P.M. Ajayan, T.W. Ebbesen, T. Ichihashi, S. Iijima, K. Tanigaki, H. Huira, Nature 362 (1993) 522.
[43] J. Liu, A.G. Rinzler, H. Dai, J.H. Hafner, R.K. Bradley, P.J. Boul, A. Lu, T. Iverson, K. Shelimov, C.B. Huffman, F. Rodriguez-Macias, Y.-S. Soon, T.R. Lee, D.T. Colbert, R.E. Smalley, Science 280 (1998) 1253.
[44] K. El-Hami, K. Mitsushige, Int. J. Nanosci. 2 (2003) 125.
[45] Z. Liu, L.C. Qin, Chem. Phys. Lett. 408 (2005) 75.